European Review for Medical and Pharmacological Sciences 2022; 26: 2259-2278

# A novel risk prediction model of pyroptosis-related genes for the prognosis and immunotherapy response of endometrial cancer

Z.-S. LIU[1], C.-L. JING[2]

[1]Department of Gynecology and Obstetrics, The First Affiliated Hospital of Dalian Medical University, Dalian, China
[2]Department of the Ultrasound of Gynecology and Obstetrics, The Second Affiliated Hospital of Dalian Medical University, Dalian, China

**Abstract. – OBJECTIVE: This study aims to develop a risk prediction model of pyroptosis-related genes based on its impact on immunotherapy sensitivity of uterine corpus endometrial carcinoma (UCEC), one of the most common and threatening gynecological malignancies.**

**PATIENTS AND METHODS: Through multiple bioinformatics analysis, we obtained raw counts of RNA-sequencing data and corresponding clinical information related to UCEC from The Cancer Genome Atlas (TCGA) and Gene Expression Profiling Interactive Analysis (GEPIA) to investigate the potential mechanisms of differentially expressed pyroptosis-related genes (DEPRGs), including the correlation between DEPRGs and prognosis, tumor immune microenvironment and the immunotherapy sensitivity of UCEC patients. Gene Ontology (GO) and Kyoto Encyclopedia of Genes and Genomes (KEGG) Enrichment Analysis were used to figure out the functional differences. Furthermore, a mRNA–miRNA–lncRNA network was constructed to identify potential impact of pyroptosis on tumor progression.**

**RESULTS: In this study, we achieved six DEPRGs (CASP3, GPX4, GSDMD, NOD2, PYCARD and TIRAP) and constructed a 6-gene signature which classified UCEC patients in the TCGA cohort into a low-risk group or a high-risk group. Patients in the low-risk group showed significantly longer survival time ($p$=0.000373). The risk score was also confirmed as an independent prognostic factor combining with the clinical characteristics. GO and KEGG functional analysis revealed the possible molecular mechanisms by which six DEPRGs influence anti-tumor immunity in UCEC patients. In addition, we found that two DEPRGs (GPX4, TIRAP) were not only significantly associated with tumor mutational burden (TMB) or microsatellite Instability (MSI), but also involved in regulating the number and function of CD8+ cells.**

**CONCLUSIONS: Upon comprehensive bioinformatics analysis, it was concluded that pyroptosis-related genes (PRGs) could predict the prognosis of EC patients and be affected in modulating the anti-tumor immune responses for patients with EC.**

*Key Words:*
Endometrial cancer, Pyroptosis-related genes, Overall survival, Prognosis, Immunotherapy response.

## Introduction

EC is among the most common gynecological malignancies in developed countries, with steady growth of incidence at approximately 1.3% each year[1]. For EC patients eligible for surgery, standard management, including total hysterectomy and bilateral salpingo-oophorectomy with surgical staging is recommended. Adjuvant therapy (chemotherapy or radiotherapy) is tailored based on the patient's pathological characteristics and clinical risk factors including age, Body Mass Index (BMI), menopause, etc. However, for patients with advanced EC who have already received standard management, effective treatment opinions are often lacking. In recent years, immunotherapy, especially immune checkpoint inhibitor (ICI) therapy, has achieved positive prognostic outcomes for a variety of solid tumors, such as non-small cell lung cancer (NSCLC)[2], hepatocellular carcinoma[3] and UCEC[4]. Therefore, immunotherapy is gradually becoming a new resort for patients with advanced malignant tumors. However, according to previous scholars[5], most tumor patients had poor response to immunotherapy. For example, Goodfellow et al[5] used pembrolizumab to treat UCEC. They found that only 20-30% of patients had MSI, and only about half of UCEC patients responded to treatment. Therefore, how to improve the sensitivity to immunotherapy has become a problem pressing for solution.

Unlike apoptosis, pyroptosis is a programmed cell lytic death caused by inflammasomes. Pyroptosis has

*Corresponding Author:* Fandou Kong, MD; e-mail: zesiliu@163.com

several distinct qualities including the cleavage of proteins such as gasdermin D (GSDMD), which could create pores in the cell membrane, its characteristic bubble-like morphology and the release of inflammatory factors[6]. There are mainly four pathways that can trigger pyroptosis, as shown in Table I.

Pyroptosis may be implicated in several diseases, including diabetes[7], atherosclerosis[8], nervous system diseases[9,10], HIV[11], and so on. Luo et al[7] reported that the presence of large amounts of NLRP3, a pyroptosis-associated inflammsome, were found in the cardiomyocytes of patients with diabetic cardiomyopathy. In addition, HIV might induce the cell death of CD4+ T cell by caspase-1-mediated pyroptosis[11]. An increasing number of studies has demonstrated the correlation of pyroptosis with the development of various solid tumors, although the role of pyroptosis in different cancer types has remained unclear. Taking GSDMD as an example, since the expression of GSDMD was positively correlated with tumor aggressiveness in NSCLC, GSDMD was regarded as a tumor promotor[12]. In contrast, GSDMD was taken as the tumor suppressor for gastric cancer, with GSDMD expression significantly downregulated[13]. Specific to the tumor immunotherapy mentioned above, there has been increasing evidence[14] that the induction of pyroptosis could improve the efficacy of immunotherapy. The study of Erkes et al[15] reported that BRAF inhibitors together with MEK inhibitors could promote cleavage of gasdermin E (GSDME) and release of HMGB1, markers of pyroptotic cell death, in melanoma with higher intratumoral T-cell infiltration. However, the specific underlying mechanisms of pyroptosis in the procession of UCEC and its impact on immunotherapy for UCEC have still rarely been reported.

Thus, we performed a systematic study to determine the expression levels of PRGs between normal and UCEC tissues using The Cancer Genome Atlas (TCGA) database. Then, we explored the prognostic value of DEPRGs and conducted a PRGs model to predict the prognosis of UCEC patients. Furthermore, we stepped forward to investigate the impact of PRGs on the tumor immune microenvironment and the immunotherapy sensitivity of UCEC patients.

## Patients and Methods

### Data Collection and Pre-Processing

For the 543 UCEC patients of TCGA database, the RNA expression and clinical data of UCEC patients were downloaded from the Genomic Data Commons (GDC) data portal (https://portal.gdc.cancer.gov/) on June 1, 2021. The clinical information of the UCEC patients was listed in Table II, while 33 pyroptosis-related genes extracted from prior reviews were shown in Table III[16-19].

### Identification of Differential Expression of Pyroptosis-related Genes

Wilcoxon signed-rank test was applied to search for differential expression genes (DEGs) between tumor tissues and normal samples employing the "ggplot2" R package. A $p < 0.05$ was considered to be statistically significant. Then, a total of 27 DEPRGs were obtained, for which the correlation map was displayed by the "corrplot" R software package. We used Spearman's correlation analysis to describe the correlation between quantitative variables without a normal distribution. STRING (https://string-db.org/), a search tool for the retrieval of interacting genes or proteins was applied to construct a protein-protein interaction (PPI) network for 27 DEGs (interaction score= 0.9).

### Development of the Pyroptosis-Related Gene Prognostic Model

A univariate Cox analysis of overall survival (OS) was performed to screen the prognostic

**Table I.** The four main pyroptosis pathways.

| Type | Triggers | Processing |
|---|---|---|
| **Canonical inflammasome pathway** | PAMP/DAMP | Activatng the inflammasomes and activated caspase 1 can cleave GSDMD and pro-IL-1β/IL-18 |
| **Non-canonical inflammasome pathway** | LPS | Binding to and activating pro-caspase 4/5 to cleave GSDMD. |
| **Chemotherapeutic drug** | disrupting the mitochondrial membrane and releasing Cyt c | activating caspase 9 and caspase 3 to cleave GSDME |
| **CTLs and NK cells** | Perforin and Gzms | GzmA and GzmB can cleave GSDMB/E |

**Notes:** PAMP: Gram-negative bacteria, viruses, toxins. DAMP: intracellular ROS, ATP, potassium, cadmium. CTLs: Cytotoxic T lymphocytes. NK cells: natural killer cells. Cyt c: cytochrome c. Gzm: granzymes

**Table II.** The clinical information of the UCEC patients.

| Total | | 543 |
|---|---|---|
| **Status (%)** | Alive | 452 (83.2) |
| | Dead | 91 (20.1) |
| **Age** | Mean (SD) | 64 (11.1) |
| | Median [MIN, MAX] | 64 [31,90] |
| **Race (%)** | AMERICAN INDIAN | 4 (0.7) |
| | ASIAN | 20 (3.9) |
| | BLACK | 106 (20.7) |
| | ISLANDER | 9 (1.7) |
| | WHITE | 372 (72.7) |
| **FIGO stage (%)** | I | 339 (65.6) |
| | II | 51 (9.8) |
| | III | 124 (24.0) |
| | IV | 29 (5.6) |
| **Grade (%)** | G1 | 98 (18.4) |
| | G2 | 120 (22.5) |
| | G3 | 314 (59.0) |
| **Tumor type (%)** | Metastasis | 37 (43.5) |
| | Primary | 11 (12.9) |
| | Recurrence | 37 (43.5) |
| **Radiation therapy (%)** | Non-radiation | 19 (28) |
| | Radiation | 31 (62) |
| **History of neoadjuvant treatment (%)** | Neoadjuvant | 2 (0.3) |
| | No neoadjuvant | 541 (99.7) |

**Notes:** FIGO: The International Federation of Gynecology and Obstetrics.

DEPRGs. Then, we conducted the least absolute shrinkage and selection operator (LASSO) regression algorithm for feature selection, using 10-fold cross-validation, to develop the prognostic model with the "glmnet" R package. For Kaplan-Meier curves, *p*-values and hazard ratio (HR) with 95% confidence interval (CI) were generated by log-rank tests and univariate Cox proportional hazards regression. We obtained six prognostic DEPRGs and corrected the gene expression levels by demographics in multivariate regression models.

Besides, the risk score was also calculated based on the following formula:

Risk score = $\sum$ (expression value of each gene × and its coefficient).

According to the median risk score, UCEC patients were divided into low- and high-risk subgroups respectively, followed by a Kaplan-Meier analysis to evaluate the predictive accuracy of each gene and risk score using the "survival" and "survminer" R packages. The "Rtsne" R package was applied to carry out a principal components analysis (PCA) to visualize the difference six gene expressions. A 1-, 3-, and 5-year receiver operating characteristic (ROC) curve analysis was conducted employing the "timeROC" R package, with a nomogram constructed to predict corresponding OS of UCEC patients, integrating our prognostic model. The expression level of 6 prognosis DEPRGs was validated in GEPIA an online database forcing on the standardized analysis of a tremendous amount of RNA sequencing data based on TCGA and GTEx data[20]. A $p<0.05$ was considered to be statistically significant.

### Functional Enrichment Analysis of the DEGs

To confirm the difference of underlying function between the high-risk group and low-risk group, we used the "clusterProfiler" R package to conduct functional enrichment. GO, including the biological process (BP), cellular component (CC), and molecular function (MF) categories, was widely employed for annotating genes with functions. KEGG Enrichment Analysis was a practical resource for the analytical study of gene functions and associated high-level genome functional information. A *p*-value less than 0.05 and an FDR less than 0.1 were considered to be statistically significant.

### Construction of Competing Endogenous RNA Network

Kruskal-Wallis test was employed to analyze the relationship between six prognostic genes and The International Federation of Gynecology and

**Table III.** The list of pyroptosis-related genes.

| | Genes |
|---|---|
| **Pyroptosis-related genes** | GPX4, NLRP7, NLRP2, CASP, CASP6, TNF, IL1B, IL18, CASP8, NLRP6 IL6, GSDMA, GSDMC, PYCARD, CASP5, AIM2, NOD2, NLRC4, NLRP3, CASP4, CASP1, PRKACA, ELANE, TIRAP, SCAF11, PJVK, CASP9, NOD1, PLCG1, NLRP1, GSDME, GSDMD, GSDMB |
| **Differentially expressed PRGs** | GPX4, NLRP7, NLRP2, CASP, CASP6, TNF, IL1B, IL18, CASP8, NLRP6 IL6, GSDMA, GSDMC, PYCARD, CASP5, AIM2, NOD2, NLRC4, NLRP3, CASP4, CASP1, PRKACA, ELANE, TIRAP, SCAF11, PJVK, CASP9, NOD1, PLCG1, NLRP1, GSDME, GSDMD, GSDMB |
| **Prognostic DEPRGs** | CASP3, GPX4, GSDMD, NOD2, PYCARD, TIRAP |
| **FIGO stage related** | DEPRGsGPX4, NOD2, PYCARD, TIRAP |

**Notes:** PRGs: pyroptosis-related genes; DEPRGS: differentially expressed pyroptosis-related genes FIGO: The International Federation of Gynecology and Obstetric.

Obstetrics (FIGO) stage. To further clarify the potential functions of DEPRGs in UCEC and investigate the association between lncRNA and miRNA, a competing endogenous RNA network of mRNA, miRNA and lncRNA was constructed. The miRNA was selected by using miRTarBase (http://mirtarbase.mbc.nctu.edu.tw) and TarBase V.8 (http://carolina.imis.athena-innovation.gr/diana_tools/web/index.php?r=tarbasev8/index).

According to identified miRNA, we used StarBase and LncBase Predicted v.2 to screen for lncRNAs targets interacting with miRNA. Then, we compared normal and tumor tissues with Wilcoxon signed-rank test to find out their differences in miRNA and lncRNAs expression. Kaplan-Meier survival analyses of miRNA and lncRNA were also conducted by the "survival" and "survminer" R packages, with $p< 0.05$ taken as statistically significant.

### Analysis of Immune Characteristics

To establish a landscape of risk scores and infiltrating immune cells, infiltration intensity was assessed through Immune Cell Abundance Identifier (immuneCellAI), by uploading the UCEC RNA-seq data[21]. We analyzed the correlation between the low- or high-risk groups and immune-cell characteristics in UCEC patients of TCGA database by Spearman correlation analysis, which is also applied to clarify the r in UCEC patients. We further delved into the correlation between six prognosis DEPRGs and TMB or MSI. A $p$-value less than 0.05 was set to be statistically significant. All statistical analyses were accomplished with R software (v4.0.3).

## Results

### Identification of DEPRGs Between Normal and Tumor Tissues in UCEC

To begin with, we investigated the differences in the expression of 33 PRGs in tumor tissues and normal samples and found out a total of 27 DEPRGs (Table III). More specifically, 12 PRGs were upregulated and 15 PRGs were downregulated in UCEC tissues (Figure 1A). Furthermore, we stepped to explore the correlation between 27 DEPRGs (Figure 1B). Based on these DEPRGs, we performed a PPI analysis with the minimum required interaction score of 0.9, which indicated that CASP8, TNF, NLRP1, IL18, CASP1 and NLRP3 were central genes (Figure 1C).

### Development of a Prognostic Gene Penal by DEPRGs

To construct a prognostic gene penal, we resorted to univariate Cox regression analysis for primary screening of the survival-related DEPRGs. As a result, the expression of 6 DEPRGs proved to be associated for the OS of UCEC patients, including CASP3 ($p$=0.046), GPX4 ($p$=0.01), GSDMD ($p$=0.043), NOD2 ($p$=0.013), PYCARD ($p$=0.045) and TIRAP ($p$=0.011), which were chosen as prognostic DEPRGs. The results of the Kaplan-Meier survival curves indicated that the six genes (CASP3, HR=0.650; GPX4, HR=0.575; GSDMD, HR=0.648; NOD2, HR=0.583; PYCARD, HR=0.653; TIRAP, HR=0.570) were protective genes with HR<1 (Figure 2). Then, we constructed a 6-gene signature by performing the least absolute shrinkage and selection operator (LASSO) Cox regression analysis and multivariate Cox analysis (Figure 3A, B). According to the formula mentioned above, the risk score of each patient was calculated as follows:

Expression value of CASP3 × (−0.1229) + expression value of GPX4 × (−0.3951) + expression value of GSDMD × (−0.1420) + expression value of NOD2 × (−0.2009) + expression value of PYCARD × (−0.0133) +expression value of TIRAP × (−0.2713)

Based on the median risk score, UCEC patients were divided into high-risk group and low-risk group. The survival status of patients within each group was presented in (Figure 3C, D). The results showed that patients in the high-risk group not only bore higher death rate but were also relatively shorter in survival cycle (Figure 3E). In the meantime, Time-dependent ROC analysis was used to assess the sensitivity and specificity of our prognostic model. The area under the ROC curve (AUC) of our model was 0.625 for 1-year survival, 0.663 for 3-year survival and 0.717 for 5-year survival (Figure 3F). We combined the prediction model with some clinicopathological characteristics, including age, BMI, histological type, FIGO stage and grade, to construct a nomogram to predict the OS of UCEC patients at 1-, 3- and 5-year stages (Figure 4).

The GEPIA database based on TCGA and GTEx data was used to verify the differences between normal and tumor samples in the expression of the six prognostic DEPRGs which was consistent with our previous findings, except for NOD2 expression (Figure 5A-F). Besides, for external validation of the predicted value of six prognostic DEPRGs, we

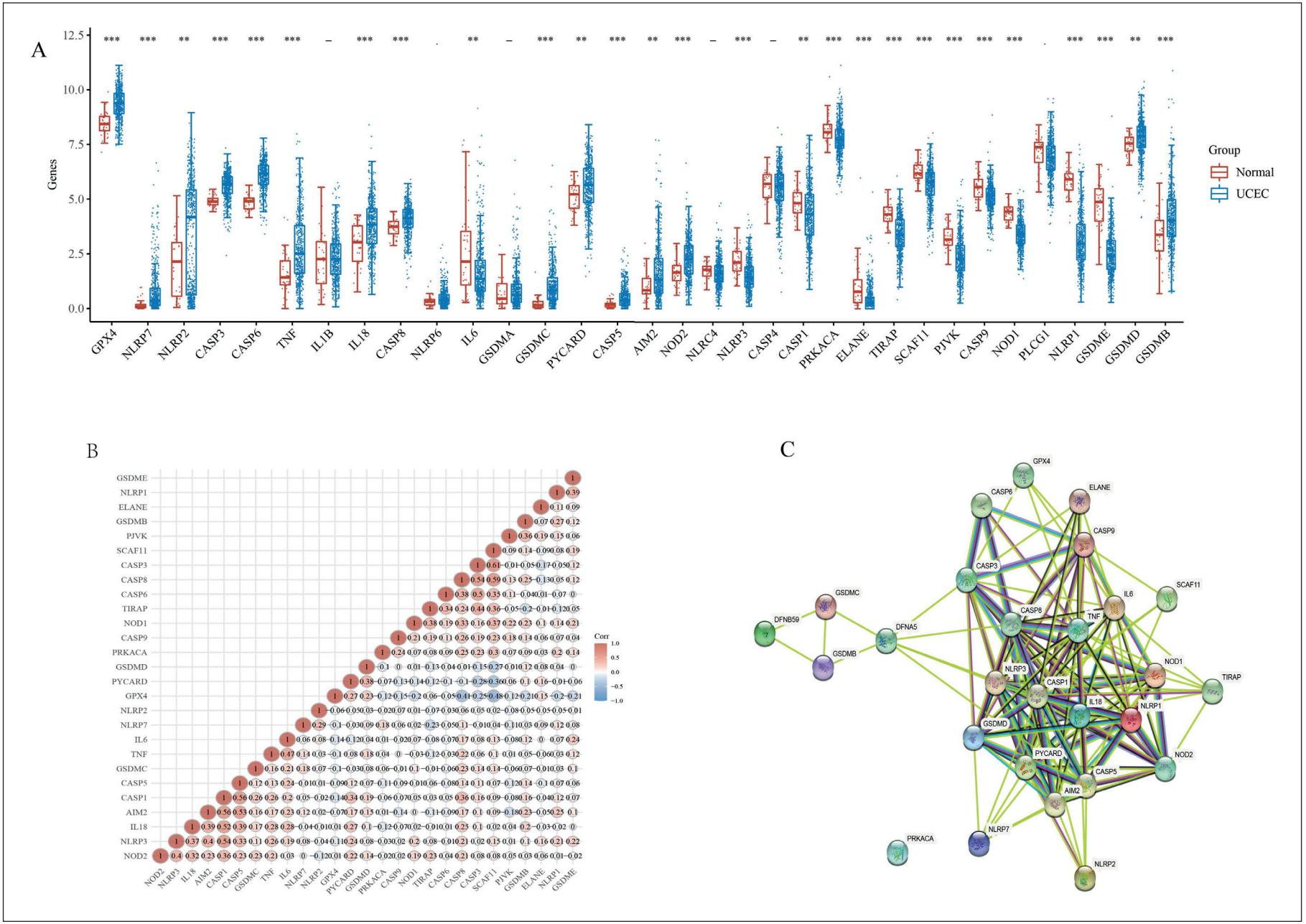


**Figure 1.** Expressions of the 33 pyroptosis-related genes and the interactions among them 27 identified DEPRGs and their expression of condition. *p*-values were showed as: $^{**}p < 0.01$; $^{***}p < 0.001$ (**A**). The correlation of the DEPRGs (**B**). PPI network showing the interactions of DEPRGs (interaction score = 0.9) (**C**).

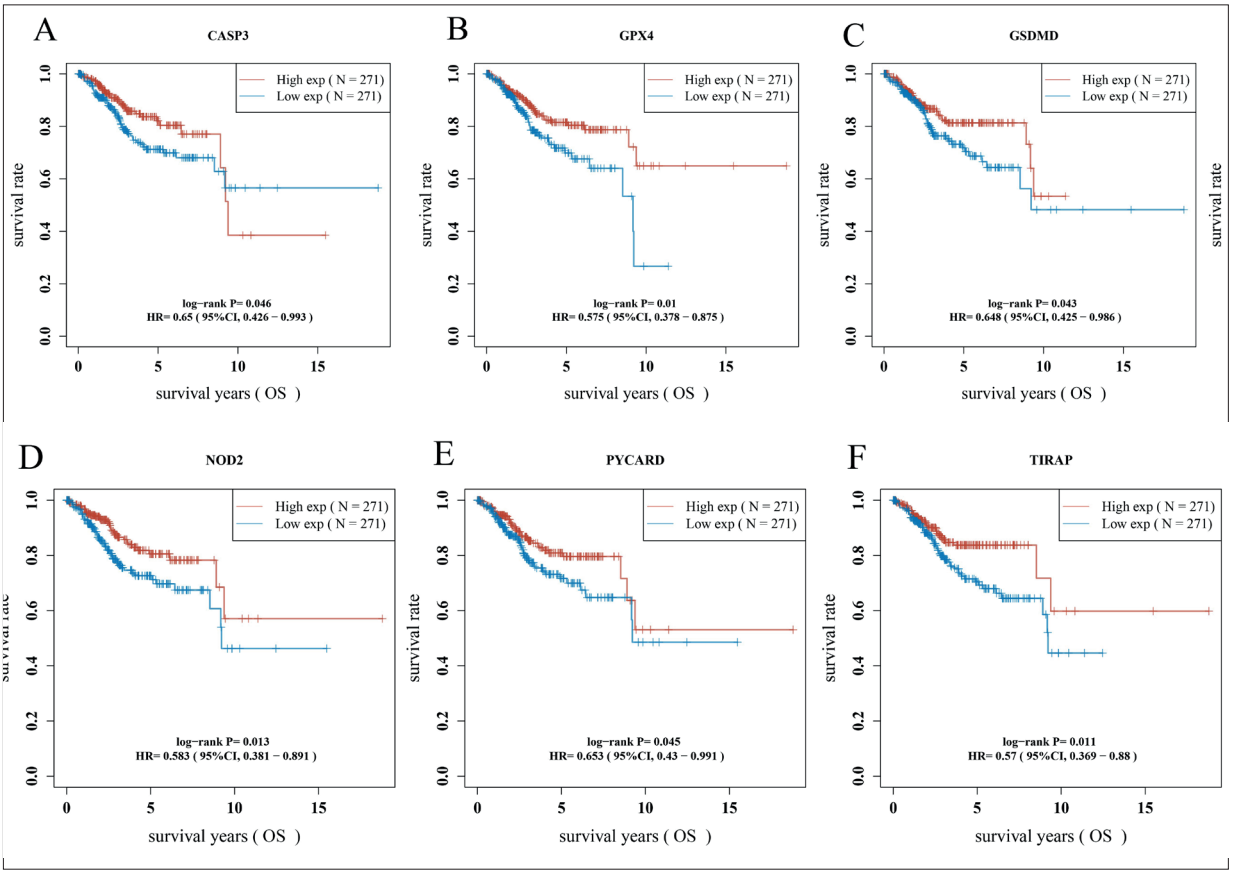


**Figure 2.** Kaplan-Meier curves for the OS of patients in the high- and low-expression of 6 prognosis DEPRGs.

analyzed the progression free survival probability (PFS) of six prognostic DEPRGs through the Kaplan-Meier plotter in UCEC. The results illustrated that UCEC patients with high expression of the six prognostic DEPRGs had higher PFS, as mentioned in previous findings (Figure 5G-L).

### *Construction of an mRNA-miRNA-LncRNA Network*

We were interested in whether the expressions of six prognosis DEPRGs were associated with the progression of UCEC. The results showed that the differences in the expression of GPX4 ($p$=0.01), NOD2 ($p$=0.0047), PYCARD ($p$=0.018) and TIRAP ($p$=8.6e-06) in different FIGO stages were statistically significant (Figure 6A-F). This may imply that these four prognostic DEPRGs were related to tumor progression in UCEC. To clarify the potential functions of four prognostic DEPRGs in tumor progression, we constructed a network of mRNA–miRNA–lncRNA interactions. Based on data from mirTarBase and TarBase V.8, we identified miR-26b-5p as the targeting miRNA binding to four prognostic DEPRGs (Figure 7A). The OS of patients with higher miR-26b-5p expression had no difference compared to patients with lower miR-26b-5p expression ($p$=0.527), although miR-26b-5p was upregulated in UCEC ($p$=0.035) (Figure 7B, C). Then, we continued to identify its upstream 11 lncRNA targets, including MIR181A1HG, LINC00847, HCG11, AC005082.1, LINC01111, NEAT1, MALAT1, WASIR2, RP1-178F10.3, LINC00665 and TUG1 (Figure 7D), and conducted a miRNA–lncRNA axis. The mRNA–miRNA–lncRNA network was shown in Figure 7I. Similarly, we made comparative analysis of differential upstream lncRNA targets expressions between the tumor and normal tissues. The results indicated that, compared with normal samples, 4 out of 11 lncRNA targets expressions were downregulated in UCEC, including HCG11 ($p$=5.8e-18), LINC00847 ($p$=3.5e-11), NEAT1 ($p$=0.0099) and TUG1 ($p$=0.0051) (Figure 7E-H). The correlation with the expressions of lncRNA targets and the OS of UCEC patients was also covered, but there appeared to be no lncRNA target that could influence the OS of UCEC patients.

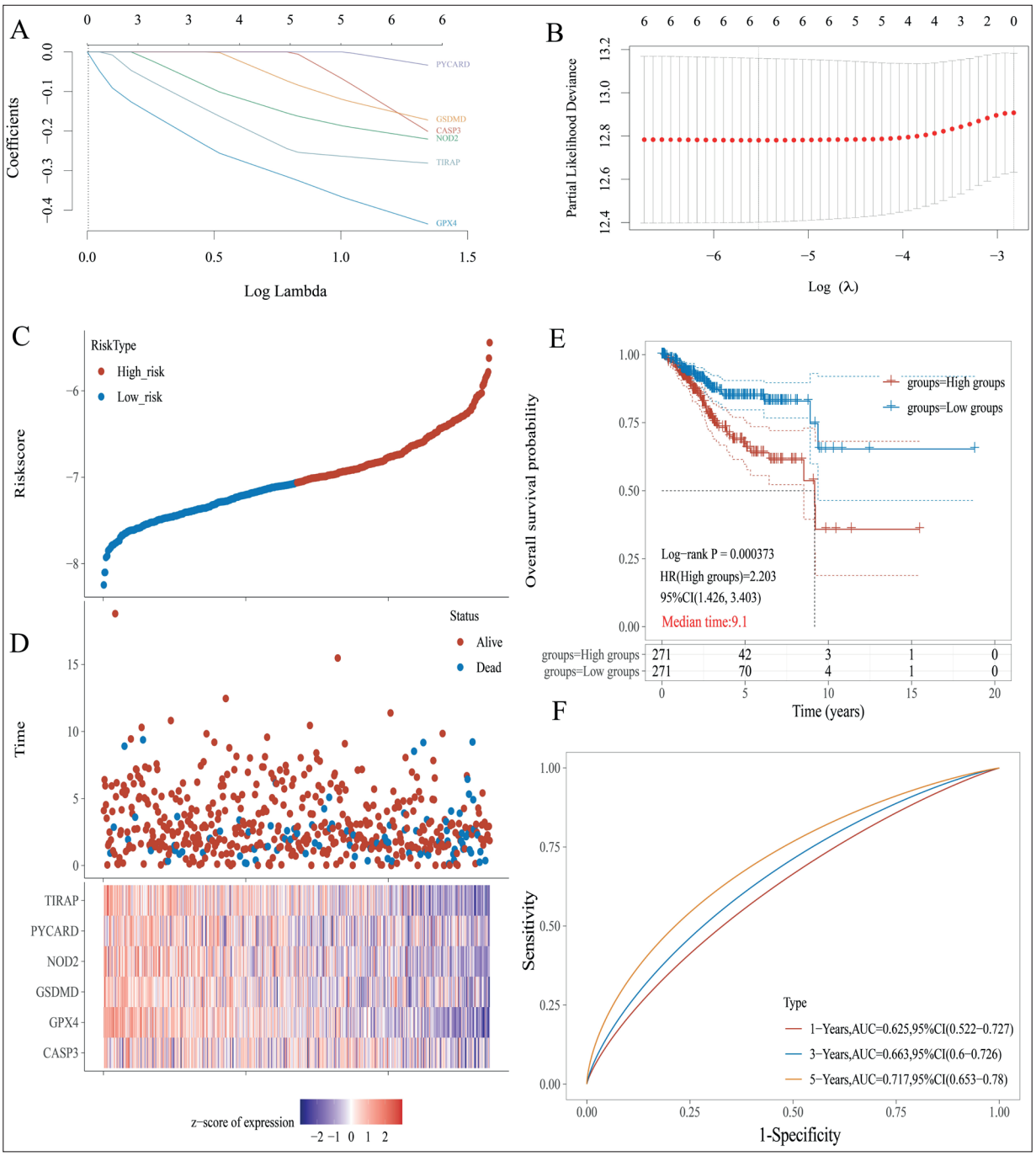


**Figure 3.** Construction of the risk panel in the TCGA cohort LASSO regression of the 6 OS-related DEPRGs (**A**). Cross-validation for tuning the parameter selection in the LASSO regression (**B**). Distribution of patients based on the risk score (**C**). The survival status for each patient (low-risk group: on the left side of the dotted line; high-risk group: on the right side of the dotted line) (**D**). Kaplan–Meier curves for the OS of patients in the high- and low-risk groups (**E**). The 1-, 3-, 5-year ROC curves demonstrated the predictive efficiency of the risk score (**F**).

### *Functional Analysis of High-risk Group and Low-risk Group*

To clarify the molecular mechanism of six prognostic DEPRGs, we carried out pathway and process enrichment analysis with the following ontology sources: GO Biological Processes, GO Cellular Components, GO Molecular Functions (Figure 8A-C) and KEGG Pathway (Figure 8D). The GO functional enrichment analysis suggested that these six prognostic DEPRGs were relevant to

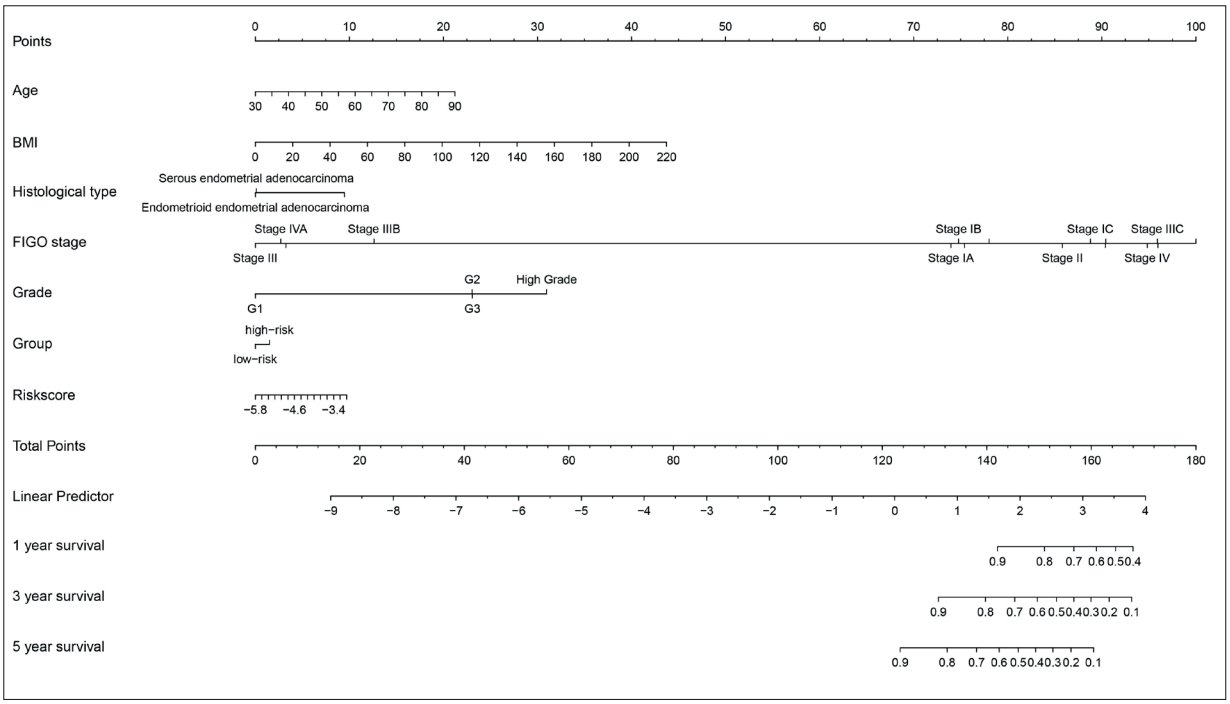


**Figure 4.** A prognostic signature-based nomogram for predicting 1-, 3-, and 5-year OS in UCEC patients.

immune response, inflammasomes production and so on. We also found that six prognostic DEPRGs were involved in the NOD-like receptor signaling pathway, PD-L1 expression and PD-1 checkpoint pathway in cancer upon KEGG analysis.

### *UCEC, Immune Checkpoint Blockade Therapy and Prognosis DEPRGs*

Based on the TIDE algorithm, we found that patients in the low-risk group had a higher TIDE score, i.e., UCEC patients in the low-risk group might be much more responsive to immune checkpoint blockade therapy compared with those in the high-risk group (Figure 9A).

To investigate the reason why patients in the high-risk group had a worse prognosis, we explored the correlation of risk score with tumor-infiltrating lymphocytes (TIL) through immuneCellAI. The results indicated that patients in the low-risk group accumulated tumor-infiltrating immune cells, such as NK cells and CD8+T cells (Figure 9B). More specifically, the risk score was negatively correlated with the infiltration of B cells (Cor=-0.17, $p$=4.43e-05), CD4+ T cells (Cor=-0.31, $p$=3.82e-13), CD8 T+ cells (Cor=-0.14, $p$=0.001), neutrophils (Cor=-0.09, $p$=0.034), macrophages (Cor=-0.18, $p$=2.68e-05), myeloid dendritic cells (Cor=-0.16, $p$=2.76e-04), macrophage M1 (Cor=-0.33, $p$=3.66e-15), NK cell (Cor=-0.10, $p$=0.0019) and endothelial cell (Cor=-0.24, $p$=8.88e-09) (Figure 10). In addition, we explored not only the correlation between the six DEPRGs and immune cells respectively, but also the relationship between tumor-infiltrating immune cells (Figure 9C, D). The mechanisms by which the risk score was correlated with the infiltration of immune cells aroused our interest. Thus, we applied a gene co-expression analysis to analyze the relationship between the expressions of each prognostic DEPRG and four immune related genes, including MHC genes, immune activation genes, chemokine related genes and chemokine receptors related genes. The results showed that PYCARD, NOD2 and GSDMD expressions were positively correlated with all MHC genes, except for HLA-DQA2 (Figure 11A). Notably, six prognostic DEPRGs were positively co-expressed with most immune activating genes, chemokine related genes and chemokine receptors related genes (Figure 11B-D).

We hypothesized that UCEC patients who have different expressions of six prognosis DEPRGs may also respond differently to ICIs therapy. Therefore, we first investigated that 6 prognosis DEPRGs were positively correlated with most of the immune checkpoints (PD-1, CD274, CTLA4, LAG3, VTCN1 and HAVCR2) (Figure 12A). Then, we investigated the correlation between

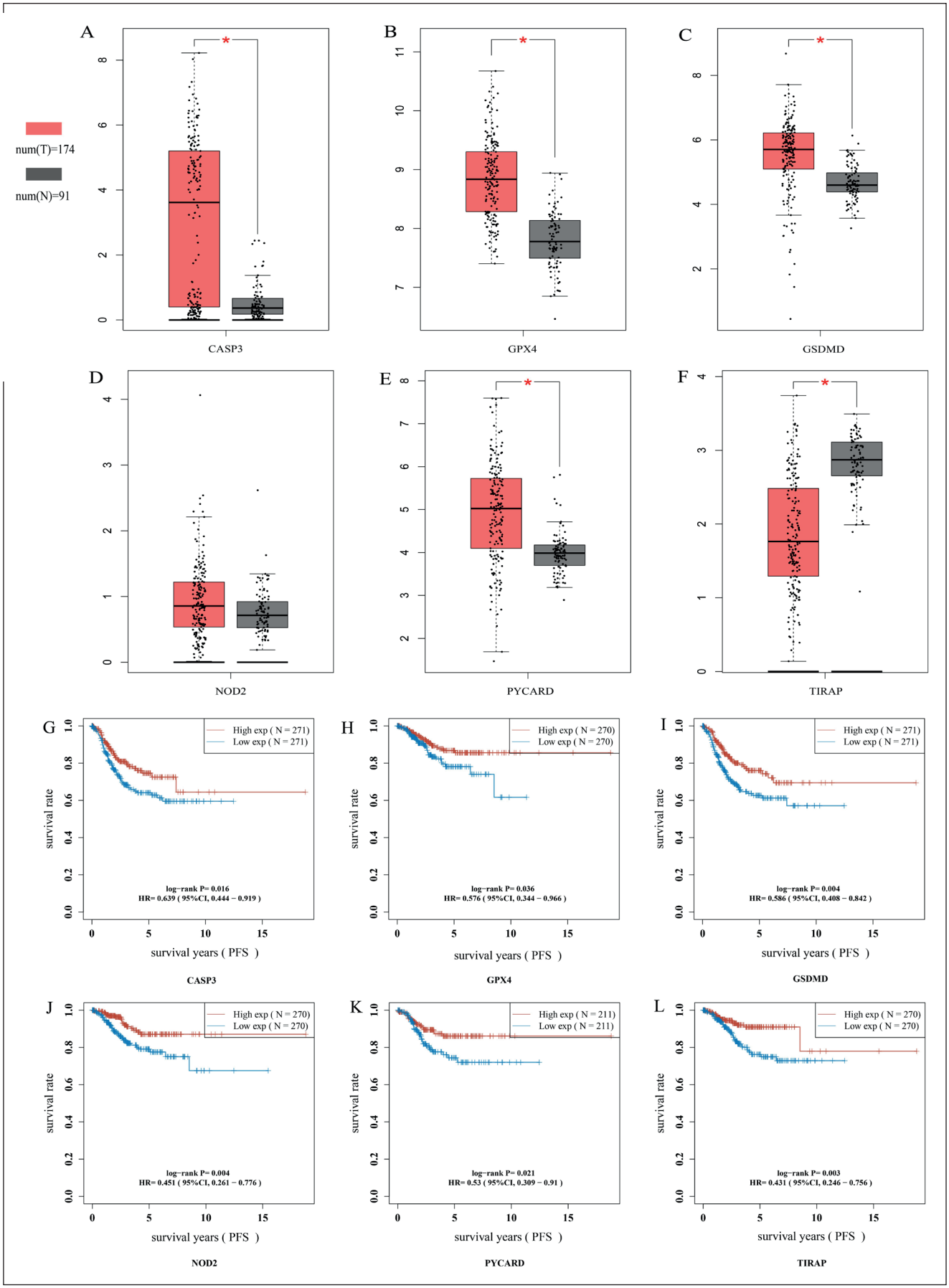


**Figure 5.** Expression and predict value validation of six prognostic DEPRGs.The expression difference (**A-F**) between EC and normal endometrial tissues based on the GEPIA database. The PFS (**G-L**) difference in groups with high or low expression of prognostic DEPRGs. *p*-values were showed as: **p* <0.05.

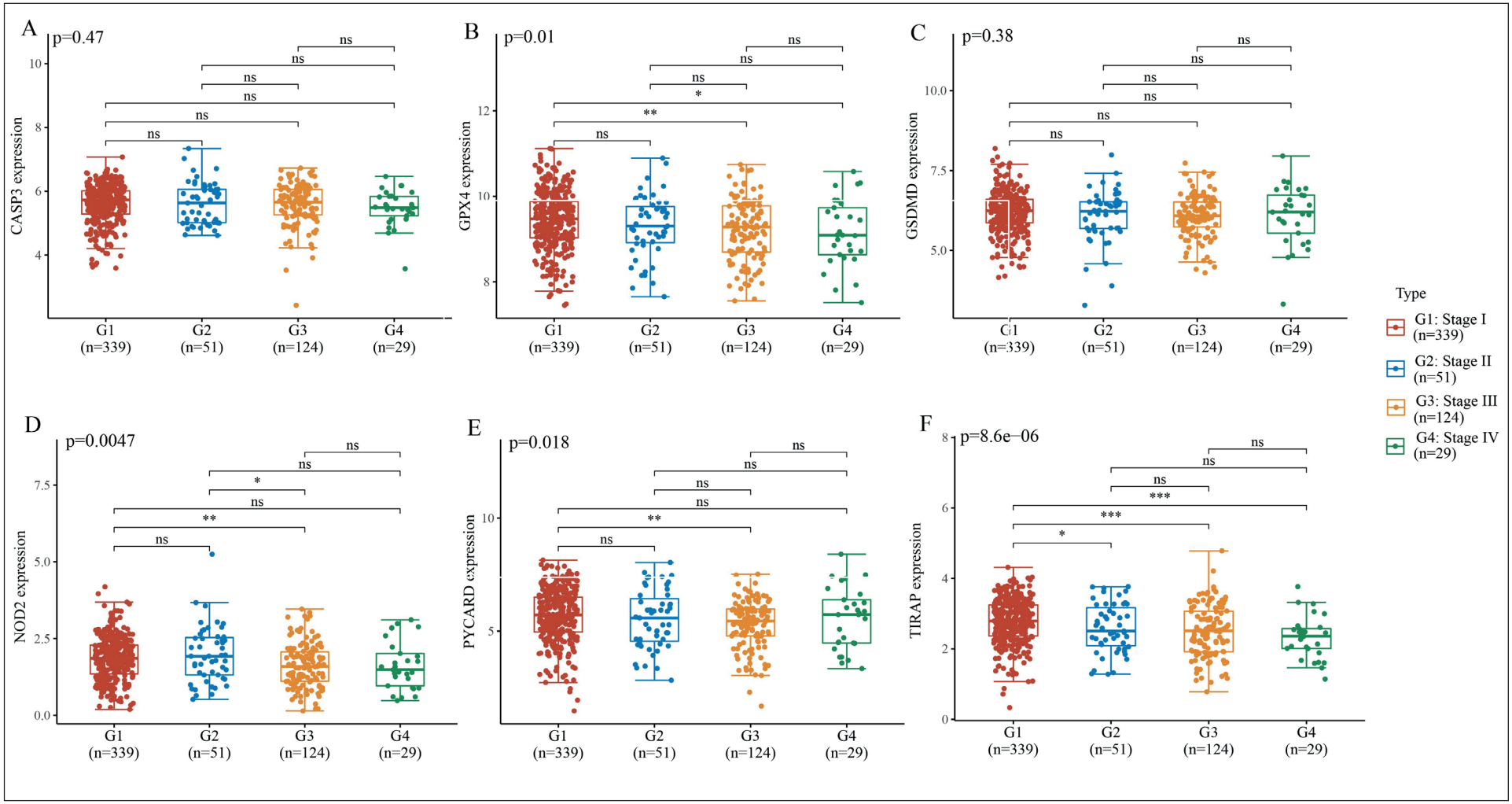


**Figure 6.** Expression of six prognostic DEPRGs in different FIGO stages. *p*-values were showed as: **p* <0.05; ***p* < 0.01; ****p* < 0.001.

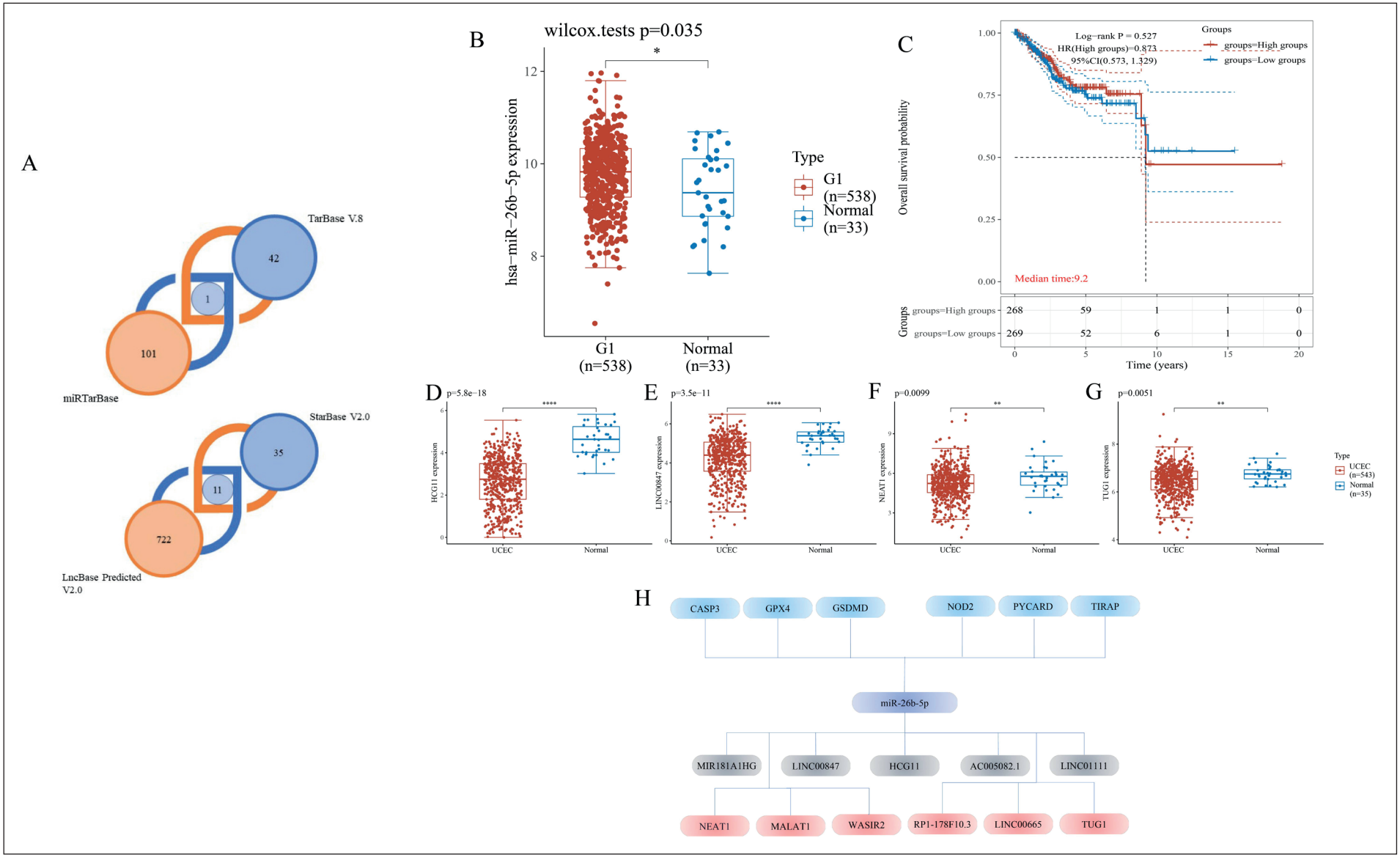


**Figure 7.** Construction of mRNA–miRNA–lncRNA network. Results of miRNA target predicted by mirTarBase and TarBase V.8 (**A**). The expression of miR-335-5p between the normal tissue and UCEC (**B**). The prognostic value of miR-335-5p in UCEC (**C**). Results of lncRNA targets predicted by lncBase predicted V.2 and StarBase V2.0 (**D**). The expression of 4 of 11 lncRNA in UCEC (**E-G**). The network of lncRNA–miRNA–mRNA (**H**).

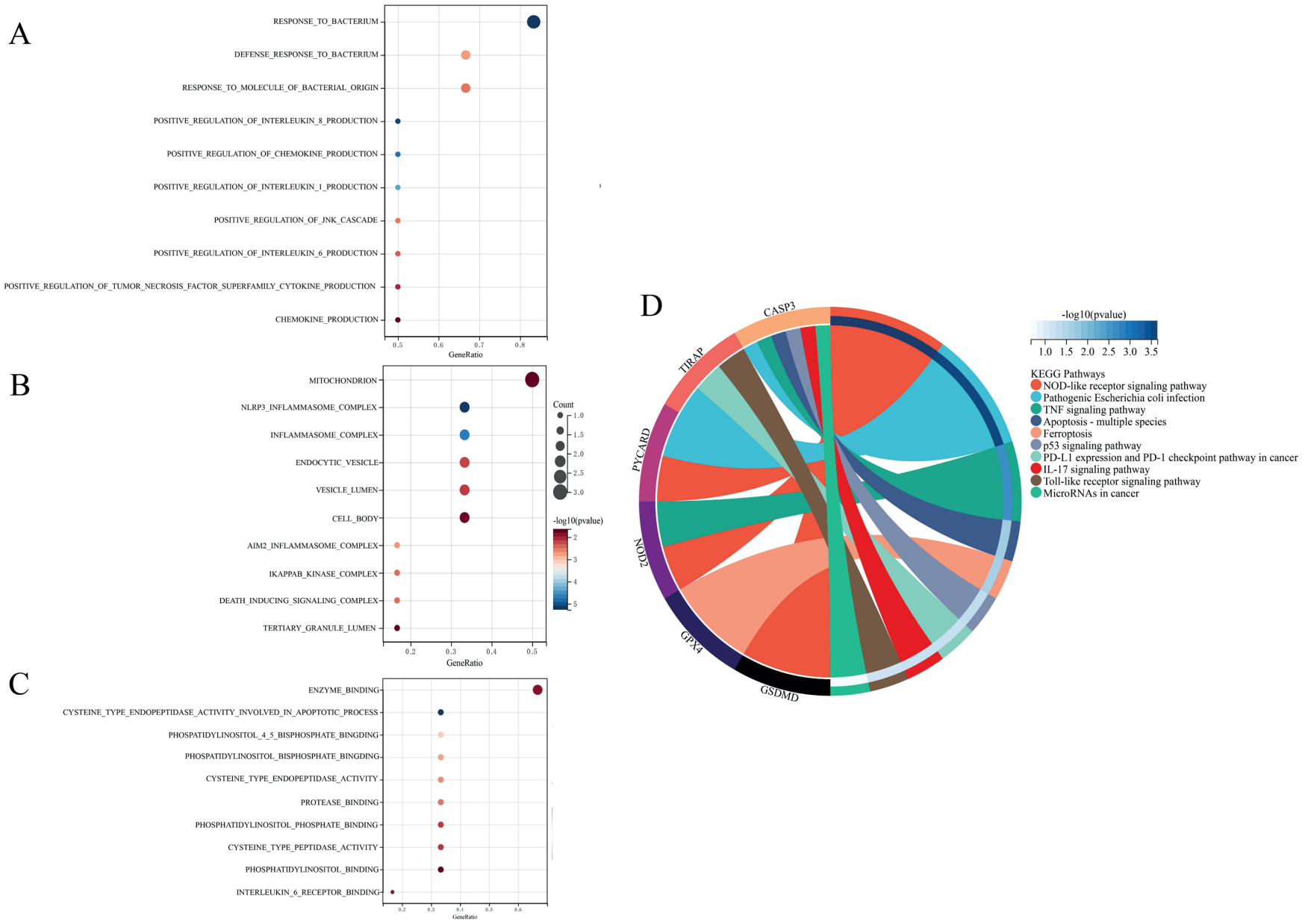


**Figure 8.** GO and KEGG functional enrichment analysis based on the six prognostic DEPRGs between the two-risk groups. Bubble graph for GO enrichment (**A-C**): the bigger bubble means the more genes enriched, and the increasing depth of color means the differences were more obvious; GO Biological Processes (**A**), GO Cellular Components (**B**), GO Molecular Functions (**C**). KEGG pathway enrichment (**D**).

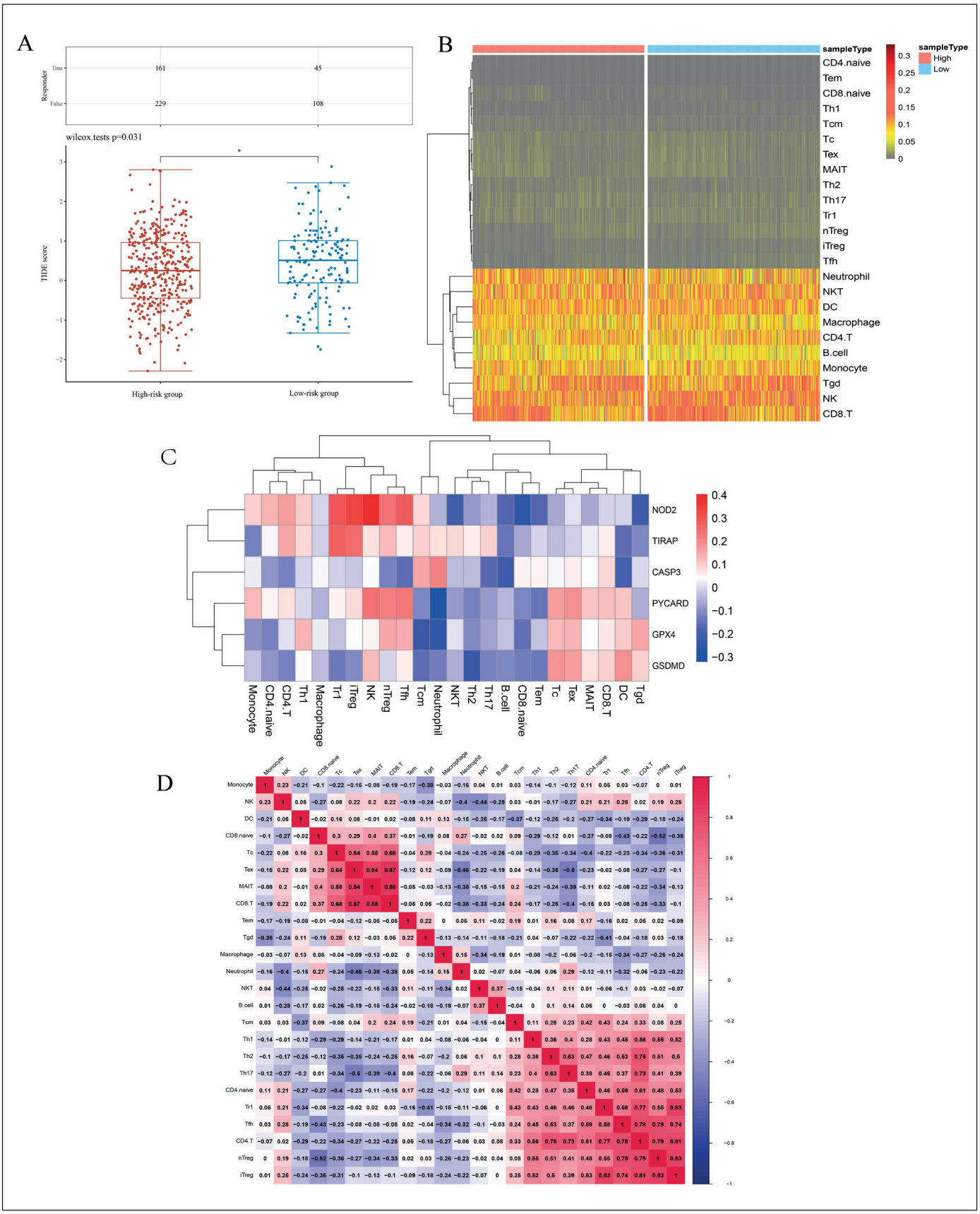


**Figure 9.** The association between the risk panel or each prognostic DEPRG and immune infiltration (immuneCellAI). The TIDE score of UCEC patients in high-and low-risk group (**A**). Heatmap for the connection between immune infiltration and the risk groups (**B**). The correlation of prognostic DEPRG and immune infiltration (**C**). The correlation of the immune cells in UCEC (**D**).

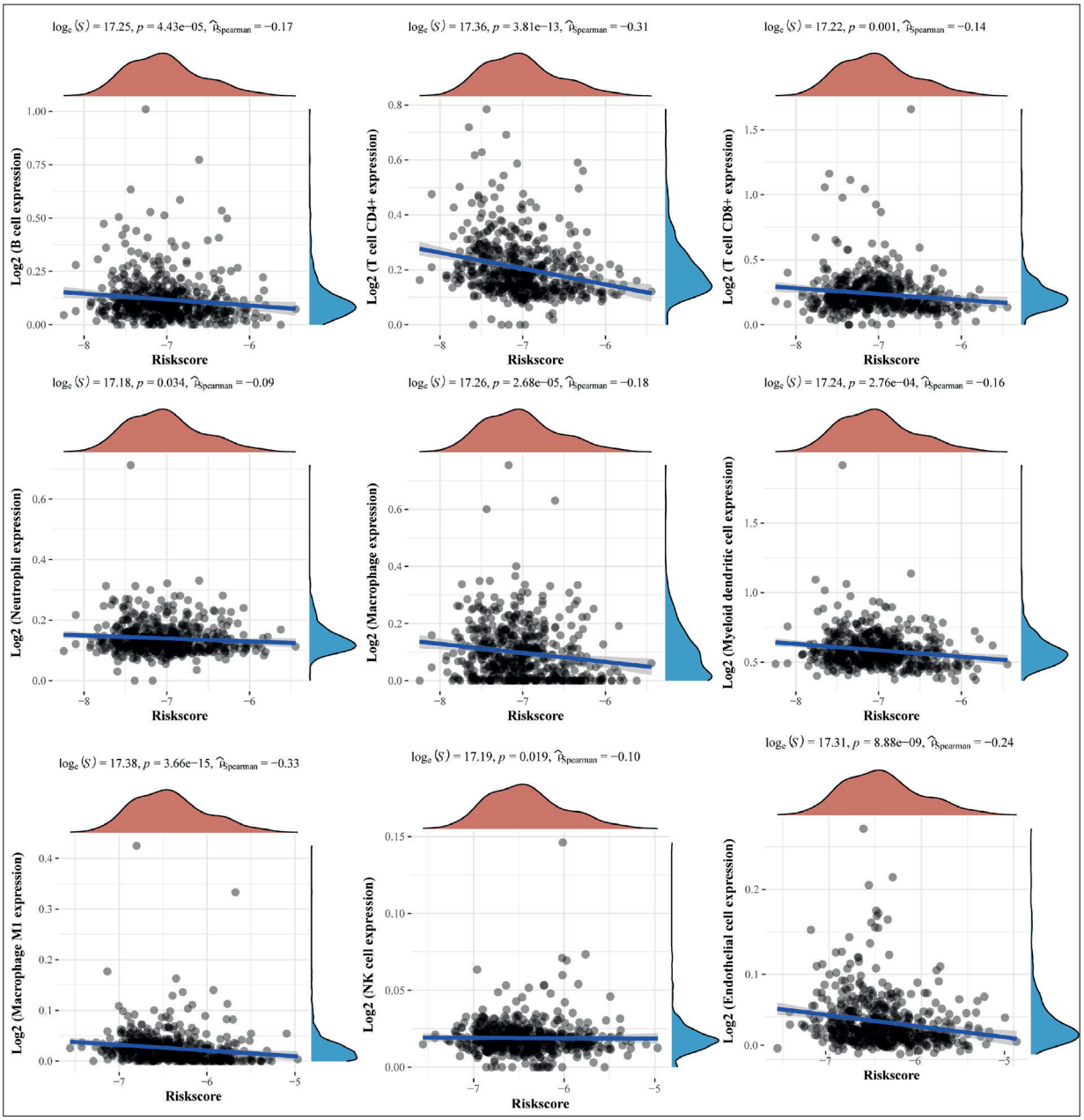


**Figure 10.** The association between the abundance of immune cells and the riskscore.

the expression of six genes and TMB as well as MSI. The results illustrated that GPX4 (Cor=0.35, *p*=1.42e-16) and TIRAP (Cor=0.29, *p*=3.46e-11) were not only positively correlated with TMB score (Figure 12C, E), but also positively related to MSI score (TIRAP: Cor=0.24, *p*=2.35e-08; GPX4: Cor=0.17, *p*=6.18e-05) (Figure 12B, D). According to a previous study[23], the expression of TCF7 and CD39 (ENTPD1) may exert an effect on CTL function. Therefore, to further investigate the mechanism of the role of these two genes in the immunotherapy of UCEC patients, the relationship between their expression and CD8+T cell, as well as three genes (TCF7, ENTPD1 and HAVCR2) associated with the function of CD8+T cells. We found that both of GPX4 (Cor=0.157, *p*=1.43e-01) and TIRAP (Cor=0.267, *p*=1.20e-02) were positively correlated with the infiltration of CD8+T cells (Figure 12F, H). At the same time, GPX4 was negatively related to the expression of

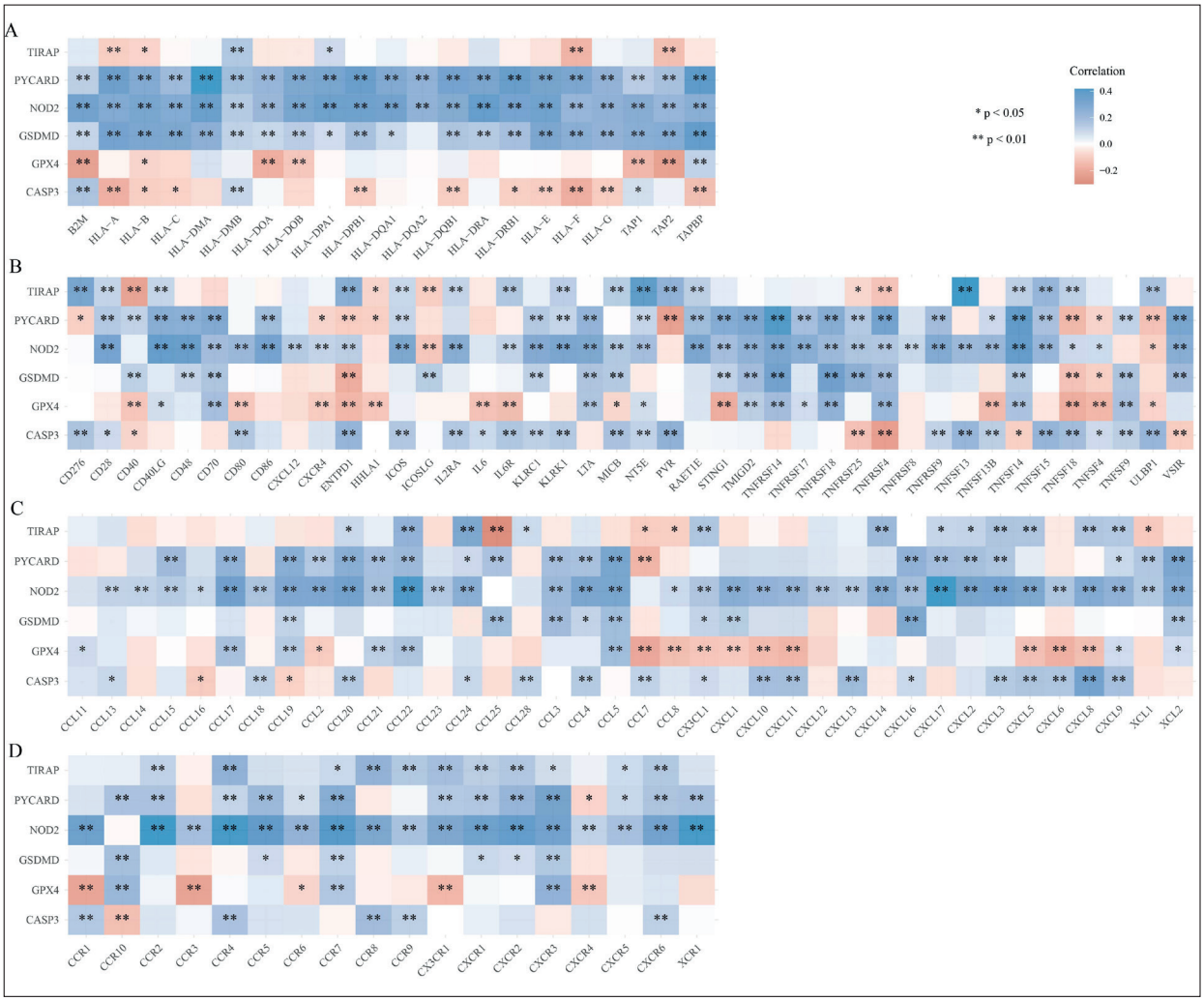


**Figure 11.** The co-expression of each prognostic DEPRG with immune-related genes. MHC related genes (**A**). Immune activation genes (**B**). Chemokine related genes (**C**). Chemokine receptors related genes (**D**).

ENTPD1 (Cor=-0.33, $p$=3.3e-06) and TIRAP was positively correlated with the expression of TCF7 (Cor=0.19, $p$=0.011) (Figure 12G, I).

## Discussion

As stated in previous studies, pyroptosis-related protein and genes were relevant to progression of various tumors, such as lung cancer[24], colorectal cancer[25], glioma[26], and so on. In recent years, the impact of pyroptosis on the development and progression of UCEC has obtained increasing attention. For example, Yang et al[27] proposed that hydrogen could inhibit endometrial cancer growth via a ROS/NLRP3/caspase-1/GSDMD-mediated pyroptotic pathway. However, there was still limited research endeavor on the impact and mechanisms of PRGs on the prognosis of UCEC.

In the present study, we compared the expression of 33 PRGs in UCEC patients in the TCGA database and identified 27 DEPRGs (including 12 upregulated PRGs and 15 downregulated PRGs). Then, we applied statistical analysis to further screen six DEPRGs (CASP3, GPX4, GSDMD, NOD2, PYCARD and TIRAP) with value for predicting prognosis in UCEC and developed a six-gene prediction panel. We found that all the genes were protective factors and patients in the low-risk group had a higher survival rate.

Previous scholars[28] suggested that the five-year survival rate of 66.9% UCEC patients diagnosed at local stage was 95%, while 16% patients with metastatic endometrial cancer were only 16.8%. This revealed significant prognosis differentiation between advanced-stage patients and early-stage ones. It is widely known that a miRNA achieves its function

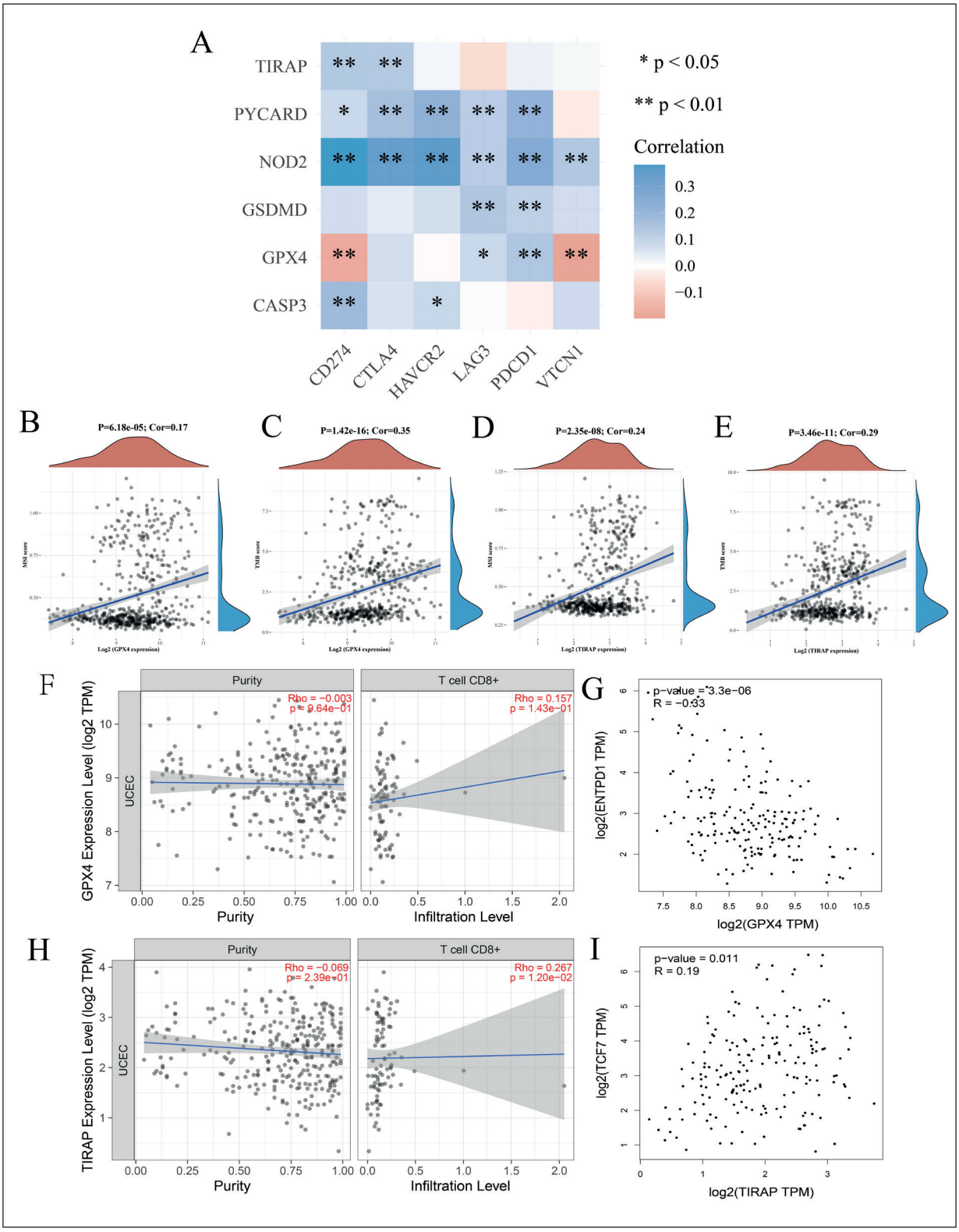


***Figure 12.*** The immune checkpoints related genes, TMB and MSI analysis of PRG in UCEC. The correlation between each prognosis DEPRG and the immune checkpoints related genes (**A**). The association between two prognosis DEPRGs (GPX4 and TIRAP) and MSI (**B**, **D**). The association between two prognosis DEPRGs (GPX4 and TIRAP) and TMB (**C**, **E**). The connection of the infiltration level of CD8+T cell and GPX4 (**F**). The connection of the infiltration level of CD8+T cell and TIRAP (**H**). The co-expression of the ENTPD1 and GPX4 (**G**). The co-expression of the TCF7 and TIRAP (**I**).

by targeting many downstream mRNA targets. For example, miRNA can interfere with tumor immunity and the microenvironment, which could possibly facilitate tumor growth, invasion, metastasis, angiogenesis and drug resistance[29]. On the other hand, abnormal changes in lncRNA expression and function might also impact the development of cancers[30]. Therefore, we attempted to explore the effect mechanism of four DEPRGs (GPX4, NOD2, PYCARD and TIRAP) associated with FIGO stage on UCEC progression by establishing a mRNA-miRNA-lncRNA network. The result showed that miR-26b-5p as a miRNA that could bind four DEPRGs was upregulated in tumor tissues and 4 out of 11 upstream lncRNAs (HCG11, LINC00847, NEAT1 and TUG1) were downregulated with the expression in UCEC, whereas we failed to find any correlation between their expression and OS of UCEC patients. This may suggest that miR-26b-5p and four lncRNAs indeed affect in the progression of UCEC, but their specific mechanisms are still in need of further study.

We conducted functional enrichment of DEPRGs between high/low-risk group in GO and KEGG. The results illustrated that "inflammasome production" and "immune and inflammatory response" had the most frequent occurrences in GO and "NOD-like receptor signaling pathway" and "PD-L1 expression and PD-1 checkpoint pathway in cancer" were enriched in the KEGG analysis, which suggested the role of immune microenvironment in UCEC prognosis.

For those patients with advanced UCEC under standard therapy, their prognostic outcomes tended to be worse due to lack of effective treatment strategies. The national comprehensive cancer network (NCCN) recommended the molecular typing of endometrial cancer of TCGA for the first time in March 2020, which suggested the dawn of a new era of genomics-based and tumor microenvironment-based immunotherapy for the treatment of endometrial cancer[31]. Unlike other gynecologic malignancies, endometrial cancer has more immune cells as well as cytokines in the tumor microenvironment (TEM), which implied those patients with endometrial cancer were more likely to benefit from immunotherapy[32,33]. At present, the main immunotherapy approaches for solid tumors included ICIs, cancer vaccines, adoptive cell transfer (ACT), and lymphocyte-promoting cytokines. Among them, ICIs therapy was regarded as one of the most effective strategies in recent years. It was in evidence suggesting that induction of pyroptosis might promote anti-tumor immunity and improve patients' sensitivity to treatment with ICIs[14,34,35]. We were hereby interested in whether the six prognosis DEPRGs would also improve the sensitivity of UCEC to ICIs therapy. We first found that the scores of the low-risk group patients were higher compared to the high-risk group patients by employing the TIDE algorithm[22], which indicated that patients in the low-risk group might be more sensitive to ICIs therapy. Currently predictive biomarkers of sensitivity to immunotherapy for UCEC mainly included immune checkpoint genes, TMB and TIL[31]. Therefore, we attempted to reveal the relevant mechanisms in each of these three terms by which six prognosis DEPRGs influence the sensitivity of UCEC to ICIs treatment.

The presence of TILs could predict better outcomes because the effector cells in TILs could exert a cytotoxic antitumor immune response in various solid tumors, such as esophageal cancer and ovarian cancer[36,37]. For patients with UCEC, the improvement of Cytotoxic T-lymphocyte (CTL) infiltration in TEM correlated with prolongation of both DPS and OS in patients[38]. Therefore, reversing the suppressive TEM is an important strategy for immunotherapy. Here we found that risk score was negatively correlated with multiple immune cells, which may explain why patients in low-risk group were associated with better prognosis. Besides, we obtained immune checkpoint genes associated with endothelial cancer from previous research[31], including PD-1, PD-L1 (CD274), CTLA4, LAG3, VTCN1 and HAVCR2. Expression of immune checkpoint genes, especially PD-L1, was significantly associated with sensitivity to ICIs treatment. Patel et al[39] reported that PD-L1-positive tumors were more effective for anti-PD-1 or anti-PD-L1 treatment (36-100%) compared to PD-L1-negative tumors (0-17%). Moreover, PD-L1 expression was upregulated in MSI-H and POLE tumors compared with MSS tumors[40]. In the current study, we first identified that six prognostic DEPRGs were positively correlated with the expression of most immune checkpoint genes. Next, we explored the relationship between six genes and MSI. The results showed that two prognosis DEPRGs (GPX4, TIRAP) were positively correlated with MSI. As with PD-L1, TMB tended to be higher in MSI-H and POLE tumors due to impaired DNA replication fidelity and defective DNA MMR system[40]. Higher TMB meant tumors can produce more neoantigens[41]. The mutation-derived neoantigens could be displayed by MHC class I on the surface of tumor cells, thus stimulating anti-tumor immunity[42]. Interestingly, we found that the two genes (GPX4, TIRAP) positively

associated with MSI were also positively associated with TMB. Since higher TMB and MSI both implied more neoantigen production, GPX4 and TIRAP appeared to promote the sensitivity to ICIs therapy by facilitating more neoantigen production. CTL played an important role in anti-tumor immunity because CTL could recognize antigens presented by MHC class I factors and kill tumor cells through releasing perforin and granzymes (Gzms) as well as expressing FasL[43]. Zhang et al[44] pointed out that GSDME expression could promote anti-tumor immunity by enhancing the number and functions of tumour-infiltrating $CD8^+$ T lymphocytes. Therefore, the relationship between GPX4 or TIRAP and CD8+ T cells aroused our interest. As a result, we found that both genes were positively associated with CD8+ T cells. Furthermore, Sade-Feldman et al[23] reported that the improvement of the proportion of TCF7+CD8+T cells suggested better efficacy of anti-PD1 therapy, and *in vivo* trials have demonstrated that inhibition of ENTPD1 could suppress tumor growth and prolong survival, which indicated that TCF7 and ENTPD1 were associated with the function and activity of CD8+ T cells. The findings in our study showed that GPX4 was negatively correlated with ENTPD1 and TIRAP was positively correlated with TCF7. This suggested that GPX4 and TIRAP not only affect the number of CTL but also take participate in the regulation of CTL function.

Previously, GPX4 has mostly been extensively studied as a gene associated with ferroptosis. Activation of GPX4 function leads to convert lipid hydroperoxides to non-toxic lipid alcohols. As a result, the formation of toxic lipid reactive oxygen species (ROS) can be prevented by this process, thus avoiding ferroptosis[45]. However, the study by Fan et al[46] also demonstrated that the expression of GPX4 is associated with pyroptosis. In the present study, we found that GPX4 not only positively correlated with TMB as well as MSI in UCEC, but also played a role in regulating the number and function of CTL in TEM, suggesting that GPX4 may influence the sensitivity of UCEC to immunotherapy through other unclear mechanisms. This may provide new hints for immunotherapy of UCEC. On the other hand, TIRAP, as Toll/Interleukin-1 receptor domain containing adaptor protein, plays an important role in the immune response[47]. But the functions it performs in tumor tissue are paradoxical. Hao et al[48] exerted anti-proliferative function through down-regulating TIRAP activity in NSCLC cells. Conversely, the findings from the study of Antosz et al[49] indicated that there may exist a defect of TIRAP proteins in B cell chronic lymphocytic leukemia (B-CLL) lymphocytes. In our study, we identified potential functions of TIRAP in the immunotherapy of UCEC, but its specific mechanism still needs to be further investigated.

## Conclusions

Altogether, our findings may contribute to clarifying the relationship between pyroptosis and immunotherapy in EC, while further research is needed to explore the underlying molecular mechanisms of pyroptosis-related pathways. External validation is also required to clarify the clinical applicability of our model.

### Acknowledgments

I would like to acknowledge my teammates for their wonderful collaboration and patient support. I would also like to thank my tutors, Fandou Kong, for their valuable guidance throughout my studies. You provided me with the tools I needed to choose the right direction and successfully complete my dissertation.

### Authorship Confirmation Statement

All authors contributed to the study conception and design. Material preparation, data collection and analysis were performed by Chunli Jing. The first draft of the manuscript was written by Zesi Liu and all authors commented on previous versions of the manuscript. All authors read and approved the final manuscript.

### Conflict of Interests

The author declare that they have no conflicts of interest.

### Funding

None.

## References

1) Lortet-Tieulent J, Ferlay J, Bray F, Jemal A. International Patterns and Trends in Endometrial Cancer Incidence, 1978-2013. J Natl Cancer Inst 2018; 4: 354-361.
2) Rizvi H, Sanchez-Vega F, La K, Chatila W, Jonsson P, Halpenny D, Plodkowski A, Long N, Sauter JL, Rekhtman N, Hollmann T, Schalper KA, Gainor JF, Shen R, Ni A, Arbour KC, Merghoub T, Wolchok J, Snyder A, Chaft JE, Kris MG, Rudin CM, Socci ND, Berger MF, Taylor BS, Zehir A, Solit DB, Arcila ME, Ladanyi M, Riely GJ, Schultz N, Hellmann MD. Molecular Determinants of Response to Anti-Programmed Cell Death (PD)-1 and Anti-Programmed Death-Ligand 1 (PD-L1) Blockade in Patients With

Non-Small-Cell Lung Cancer Profiled With Targeted Next-Generation Sequencing. J Clin Oncol 2018; 7: 633-641.

3) Federico P, Petrillo A, Giordano P, Bosso D, Fabbrocini A, Ottaviano M, Rosanova M, Silvestri A, Tufo A, Cozzolino A, Daniele B. Immune Checkpoint Inhibitors in Hepatocellular Carcinoma: Current Status and Novel Perspectives. Cancers (Basel) 2020; 12: 3025.
4) Le DT, Uram JN, Wang H, Bartlett BR, Kemberling H, Eyring AD, Skora AD, Luber BS, Azad NS, Laheru D, Biedrzycki B, Donehower RC, Zaheer A, Fisher GA, Crocenzi TS, Lee JJ, Duffy SM, Goldberg RM, de la Chapelle A, Koshiji M, Bhaijee F, Huebner T, Hruban RH, Wood LD, Cuka N, Pardoll DM, Papadopoulos N, Kinzler KW, Zhou S, Cornish TC, Taube JM, Anders RA, Eshleman JR, Vogelstein B, Diaz LA, Jr. PD-1 Blockade in Tumors with Mismatch-Repair Deficiency. N Engl J Med 2015; 26: 2509-2520.
5) Goodfellow PJ, Billingsley CC, Lankes HA, Ali S, Cohn DE, Broaddus RJ, Ramirez N, Pritchard CC, Hampel H, Chassen AS, Simmons LV, Schmidt AP, Gao F, Brinton LA, Backes F, Landrum LM, Geller MA, DiSilvestro PA, Pearl ML, Lele SB, Powell MA, Zaino RJ, Mutch D. Combined Microsatellite Instability, MLH1 Methylation Analysis, and Immunohistochemistry for Lynch Syndrome Screening in Endometrial Cancers From GOG210: An NRG Oncology and Gynecologic Oncology Group Study. J Clin Oncol 2015; 36: 4301-4308.
6) Lu X, Guo T, Zhang X. Pyroptosis in Cancer: Friend or Foe? Cancers 2021; 13, 3620.
7) Luo B, Huang F, Liu Y, Liang Y, Wei Z, Ke H, Zeng Z, Huang W, He Y. NLRP3 Inflammasome as a Molecular Marker in Diabetic Cardiomyopathy. Front Physiol 2017; 519.
8) Wu X, Zhang H, Qi W, Zhang Y, Li J, Li Z, Lin Y, Bai X, Liu X, Chen X, Yang H, Xu C, Zhang Y, Yang B. Nicotine promotes atherosclerosis via ROS-NLRP3-mediated endothelial cell pyroptosis. Cell Death Dis 2018; 2: 171.
9) Wang S, Yuan YH, Chen NH, Wang HB. The mechanisms of NLRP3 inflammasome/pyroptosis activation and their role in Parkinson's disease. Int Immunopharmacol 2019; 458-464.
10) McKenzie BA, Mamik MK, Saito LB, Boghozian R, Monaco MC, Major EO, Lu JQ, Branton WG, Power C. Caspase-1 inhibition prevents glial inflammasome activation and pyroptosis in models of multiple sclerosis. Proc Natl Acad Sci U S A 2018; 26: E6065-e74.
11) Doitsh G, Galloway NL, Geng X, Yang Z, Monroe KM, Zepeda O, Hunt PW, Hatano H, Sowinski S, Muñoz-Arias I, Greene WC. Cell death by pyroptosis drives CD4 T-cell depletion in HIV-1 infection. Nature 2014; 7484: 509-514.
12) Gao J, Qiu X, Xi G, Liu H, Zhang F, Lv T, Song Y. Downregulation of GSDMD attenuates tumor proliferation via the intrinsic mitochondrial apoptotic pathway and inhibition of EGFR/Akt signaling and predicts a good prognosis in non-small cell lung cancer. Oncol Rep 2018; 4: 1971-1984.
13) Wang WJ, Chen D, Jiang MZ, Xu B, Li XW, Chu Y, Zhang YJ, Mao R, Liang J, Fan DM. Downregulation of gasdermin D promotes gastric cancer proliferation by regulating cell cycle-related proteins. J Dig Dis 2018; 2: 74-83.
14) Wang Q, Wang Y, Ding J, Wang C, Zhou X, Gao W, Huang H, Shao F, Liu Z. A bioorthogonal system reveals antitumour immune function of pyroptosis. Nature 2020; 7799: 421-426.
15) Erkes DA, Cai W, Sanchez IM, Purwin TJ, Rogers C, Field CO, Berger AC, Hartsough EJ, Rodeck U, Alnemri ES, Aplin AE. Mutant BRAF and MEK Inhibitors Regulate the Tumor Immune Microenvironment via Pyroptosis. Cancer Discov 2020; 2: 254-269.
16) Xia X, Wang X, Cheng Z, Qin W, Lei L, Jiang J, Hu J. The role of pyroptosis in cancer: pro-cancer or pro-"host"? Cell Death Dis 2019; 9: 650.
17) Karki R, Kanneganti TD. Diverging inflammasome signals in tumorigenesis and potential targeting. Nat Rev Cancer 2019; 4: 197-214.
18) Wang B, Yin Q. AIM2 inflammasome activation and regulation: A structural perspective. J Struct Biol 2017; 3: 279-282.
19) Man SM, Kanneganti TD. Regulation of inflammasome activation. Immunol Rev 2015; 1: 6-21.
20) Tang Z, Li C, Kang B, Gao G, Li C, Zhang Z. GEPIA: a web server for cancer and normal gene expression profiling and interactive analyses. Nucleic Acids Res 2017; W1: W98-w102.
21) Miao YR, Zhang Q, Lei Q, Luo M, Xie GY, Wang H, Guo AY. ImmuCellAI: A Unique Method for Comprehensive T-Cell Subsets Abundance Prediction and its Application in Cancer Immunotherapy. Adv Sci (Weinh) 2020; 7: 1902880.
22) Jiang P, Gu S, Pan D, Fu J, Sahu A, Hu X, Li Z, Traugh N, Bu X, Li B, Liu J, Freeman GJ, Brown MA, Wucherpfennig KW, Liu XS. Signatures of T cell dysfunction and exclusion predict cancer immunotherapy response. Nat Med 2018; 10: 1550-1558.
23) Sade-Feldman M, Yizhak K, Bjorgaard SL, Ray JP, de Boer CG, Jenkins RW, Lieb DJ, Chen JH, Frederick DT, Barzily-Rokni M, Freeman SS, Reuben A, Hoover PJ, Villani AC, Ivanova E, Portell A, Lizotte PH, Aref AR, Eliane JP, Hammond MR, Vitzthum H, Blackmon SM, Li B, Gopalakrishnan V, Reddy SM, Cooper ZA, Paweletz CP, Barbie DA, Stemmer-Rachamimov A, Flaherty KT, Wargo JA, Boland GM, Sullivan RJ, Getz G, Hacohen N. Defining T Cell States Associated with Response to Checkpoint Immunotherapy in Melanoma. Cell 2019; 2: 404.
24) Wang Y, Kong H, Zeng X, Liu W, Wang Z, Yan X, Wang H, Xie W. Activation of NLRP3 inflammasome enhances the proliferation and migration of A549 lung cancer cells. Oncol Rep 2016; 4: 2053-2064
25) Wang H, Wang Y, Du Q, Lu P, Fan H, Lu J, Hu R. Inflammasome-independent NLRP3 is required for epithelial-mesenchymal transition in colon cancer cells. Exp Cell Res. 2016; 2: 184-192.

26) Li L, Liu Y. Aging-related gene signature regulated by Nlrp3 predicts glioma progression. Am J Cancer Res 2015; 1: 442-449

27) Yang Y, Liu PY, Bao W, Chen SJ, Wu FS, Zhu PY. Hydrogen inhibits endometrial cancer growth via a ROS/NLRP3/caspase-1/GSDMD-mediated pyroptotic pathway. BMC Cancer 2020; 1: 28.

28) Connor EV, Rose PG. Management Strategies for Recurrent Endometrial Cancer. Expert Rev Anticancer Ther 2018; 9: 873-885.

29) Sun Z, Shi K, Yang S, Liu J, Zhou Q, Wang G, Song J, Li Z, Zhang Z, Yuan W. Effect of exosomal miRNA on cancer biology and clinical applications. Mol Cancer 2018; 1: 147.

30) Bhan A, Soleimani M, Mandal SS. Long Noncoding RNA and Cancer: A New Paradigm. Cancer Res 2017; 15: 3965-3981.

31) Cao W, Ma X, Fischer JV, Sun C, Kong B, Zhang Q. Immunotherapy in endometrial cancer: rationale, practice and perspectives. Biomark Res 2021; 1: 49.

32) Nishio H, Iwata T, Aoki D. Current status of cancer immunotherapy for gynecologic malignancies. Jpn J Clin Oncol 2021; 2: 167-172.

33) Di Tucci C, Schiavi MC, Faiano P, D'Oria O, Prata G, Sciuga V, Giannini A, Palaia I, Muzii L, Benedetti Panici P. Therapeutic vaccines and immune checkpoints inhibition options for gynecological cancers. Crit Rev Oncol Hematol 2018; 30-42.

34) Zhou Z, He H, Wang K, Shi X, Wang Y, Su Y, Wang Y, Li D, Liu W, Zhang Y, Shen L, Han W, Shen L, Ding J, Shao F. Granzyme A from cytotoxic lymphocytes cleaves GSDMB to trigger pyroptosis in target cells. Science 2020; 368: eaaz7548.

35) Liu Y, Fang Y, Chen X, Wang Z, Liang X, Zhang T, Liu M, Zhou N, Lv J, Tang K, Xie J, Gao Y, Cheng F, Zhou Y, Zhang Z, Hu Y, Zhang X, Gao Q, Zhang Y, Huang B. Gasdermin E-mediated target cell pyroptosis by CAR T cells triggers cytokine release syndrome. Sci Immunol 2020; 43: 134-156

36) Sudo T, Nishida R, Kawahara A, Saisho K, Mimori K, Yamada A, Mizoguchi A, Kadoya K, Matono S, Mori N, Tanaka T, Akagi Y. Clinical Impact of Tumor-Infiltrating Lymphocytes in Esophageal Squamous Cell Carcinoma. Ann Surg Oncol 2017; 12: 3763-3770.

37) Sato E, Olson SH, Ahn J, Bundy B, Nishikawa H, Qian F, Jungbluth AA, Frosina D, Gnjatic S, Ambrosone C, Kepner J, Odunsi T, Ritter G, Lele S, Chen YT, Ohtani H, Old LJ, Odunsi K. Intraepithelial CD8+ tumor-infiltrating lymphocytes and a high CD8+/regulatory T cell ratio are associated with favorable prognosis in ovarian cancer. Proc Natl Acad Sci U S A 2005; 51: 18538-18543.

38) de Jong RA, Leffers N, Boezen HM, ten Hoor KA, van der Zee AG, Hollema H, Nijman HW. Presence of tumor-infiltrating lymphocytes is an independent prognostic factor in type I and II endometrial cancer. Gynecol Oncol 2009; 1: 105-110.

39) Patel SP, Kurzrock R. PD-L1 Expression as a Predictive Biomarker in Cancer Immunotherapy. Mol Cancer Ther 2015; 4: 847-856.

40) Pakish JB, Zhang Q, Chen Z, Liang H, Chisholm GB, Yuan Y, Mok SC, Broaddus RR, Lu KH, Yates MS. Immune Microenvironment in Microsatellite-Instable Endometrial Cancers: Hereditary or Sporadic Origin Matters. Clin Cancer Res 2017; 15: 4473-4481.

41) Perumal D, Imai N, Laganà A, Finnigan J, Melnekoff D, Leshchenko VV, Solovyov A, Madduri D, Chari A, Cho HJ, Dudley JT, Brody JD, Jagannath S, Greenbaum B, Gnjatic S, Bhardwaj N, Parekh S. Mutation-derived Neoantigen-specific T-cell Responses in Multiple Myeloma. Clin Cancer Res 2020; 2: 450-464.

42) Segal NH, Parsons DW, Peggs KS, Velculescu V, Kinzler KW, Vogelstein B, Allison JP. Epitope landscape in breast and colorectal cancer. Cancer Res 2008; 3: 889-892.

43) Reiser J, Banerjee A. Effector, Memory, and Dysfunctional CD8(+) T Cell Fates in the Antitumor Immune Response. J Immunol Res 2016; 8941260.

44) Zhang Z, Zhang Y, Xia S, Kong Q, Li S, Liu X, Junqueira C, Meza-Sosa KF, Mok TMY, Ansara J, Sengupta S, Yao Y, Wu H, Lieberman J. Gasdermin E suppresses tumour growth by activating anti-tumour immunity. Nature 2020; 7799: 415-420.

45) Forcina GC, Dixon SJ. GPX4 at the Crossroads of Lipid Homeostasis and Ferroptosis. Proteomics 2019; 18: e1800311.

46) Fan R, Sui J, Dong X, Jing B, Gao Z. Wedelolactone alleviates acute pancreatitis and associated lung injury via GPX4 mediated suppression of pyroptosis and ferroptosis. Free Radic Biol Med 2021; 29-40.

47) Belhaouane I, Hoffmann E, Chamaillard M, Brodin P, Machelart A. Paradoxical Roles of the MAL/Tirap Adaptor in Pathologies. Front Immunol 2020; 569127.

48) Hao S, Li S, Wang J, Yan Y, Ai X, Zhang J, Ren Y, Wu T, Liu L, Wang C. Phycocyanin Exerts Anti-Proliferative Effects through Down-Regulating TIRAP/NF-κB Activity in Human Non-Small Cell Lung Cancer Cells. Cells 2019; 6: 67-89

49) Antosz H, Sajewicz J, Marzec-Kotarska B, Dmoszyńska A, Baszak J, Jargiełło-Baszak M. Aberrant TIRAP and MyD88 expression in B-cell chronic lymphocytic leukemia. Blood Cells Mol Dis 2013; 1: 48-55.